PS Integer Experiment: Benchmarking of MAD-X SC and PyOrbit

M. Titze

Special thanks to:
H. Bartosik, A. Huschauer and F. Schmidt

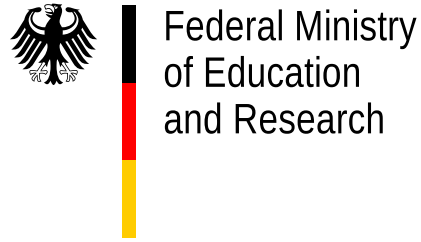

05.10.2017

Motivation

Topic: Emittance evolution in the context of direct space charge, predicted by five different space charge solvers.

Two of them are coming from MAD-X and three of them from PyOrbit:

- MAD-X SC. Both analytical (Basettie-Erskine), can run in: frozen and adaptive mode.
- PyOrbit: One analytical (Basettie-Erskine, similar to MAD-X frozen) and two PIC Codes: A 2p5d model and a 'slice-by-slice' (sbs) model.

MAD-X internal emittance vs. RMS emittance

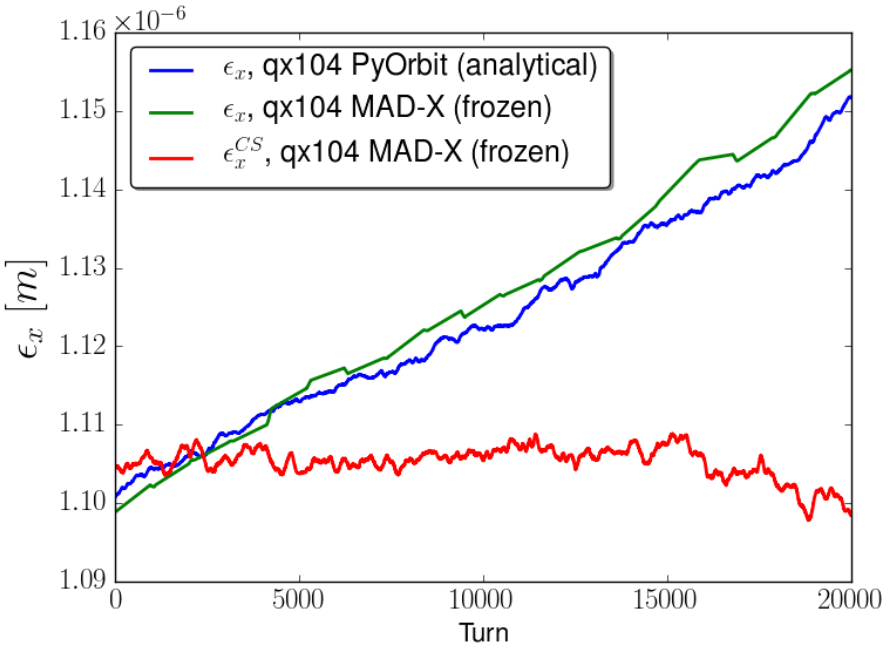

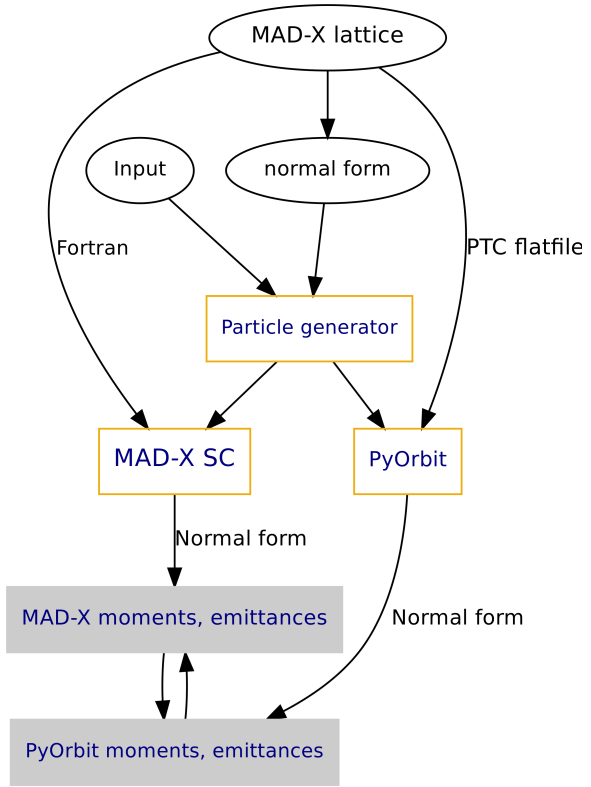

Figure 1: Left: Reminder: MAD-X internal emittance $\neq$ RMS emittance. Result of PS simulation while crossing 3rd order sextupole-driven resonance. Right: New post-analysis scheme for benchmarking both codes.

Emittance calculation from simulation

- Obtain the covariance matrix G of the distribution and the (linear) normal form map N of the lattice.
- Find $\tilde{G}$, covariance matrix & closest to G, with $M\tilde{G}M^{tr} = \tilde{G}$, where M is the (linear part of) the one-turn map.
- By the above condition: $\tilde{G} = N^{tr}DN$, where $D = \mathrm{diag}(\Lambda, \Lambda)$ and Λ is diagonal, containing the three emittances ϵ_x, ϵ_y and ϵ_z.

Emittance calculation from measurement

Two ways:

1. Via twiss parameters, assuming (uncorrelated) random variables:

$$\epsilon_x = \frac{1}{\beta_x}[\sigma_x^2 - [\Delta p/p]_{rms}^2 D_x^2]$$

2. By inverting the map

$$(\epsilon_x, \epsilon_y, \epsilon_z) \mapsto ((M_H \tilde{G} M_H^{tr})_{11}, (M_V \tilde{G} M_V^{tr})_{11}, \tilde{G}_{33}) = (b_x, b_y, b_z),$$

where M_H and M_V are the sectormaps from the lattice start to the position of the horizontal- and vertical wirescanners and (b_x, b_y, b_z) are the measured RMS values on these instruments.

Basic principle

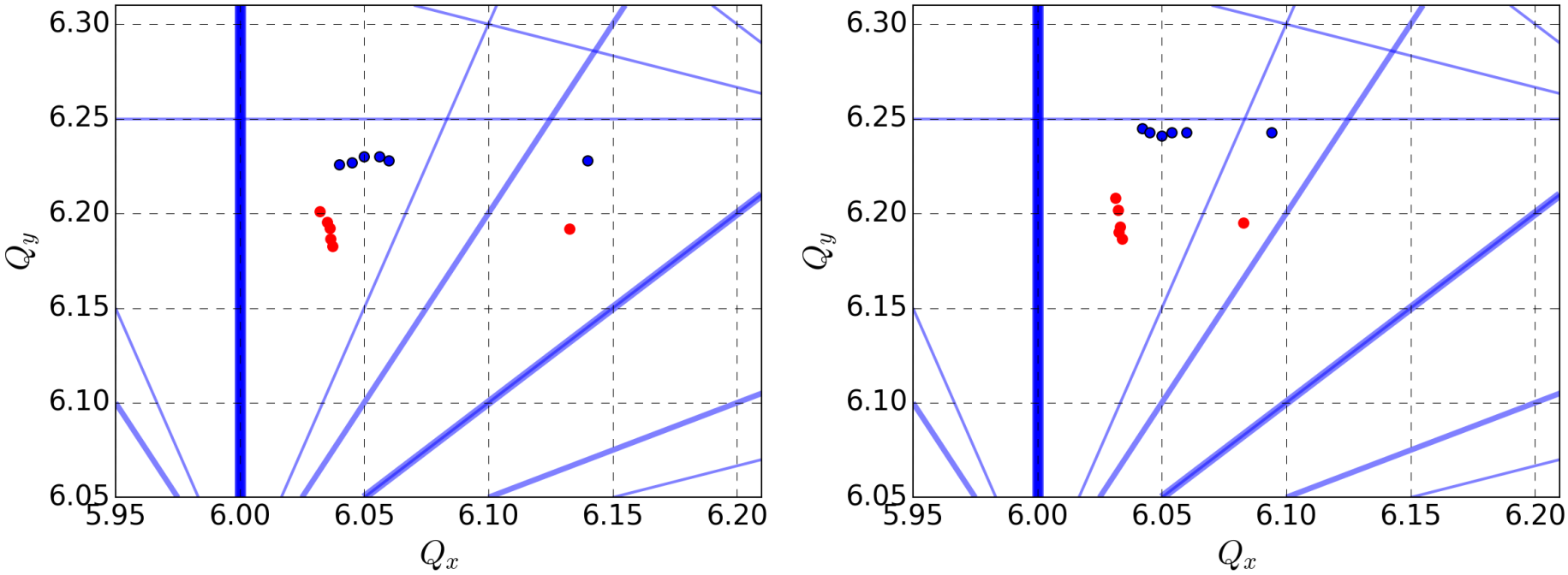

Figure 2: Tune diagrams of both measurement campaigns, left: $20 \cdot 10^{10}$ setup, right: $30 \cdot 10^{10}$ setup. Colors: Measured tune (bare tune in MAD-X) and from last `TWISS` in MAD-X SC. Resonance lines shown up to order 4.

Basic principle, p. 2

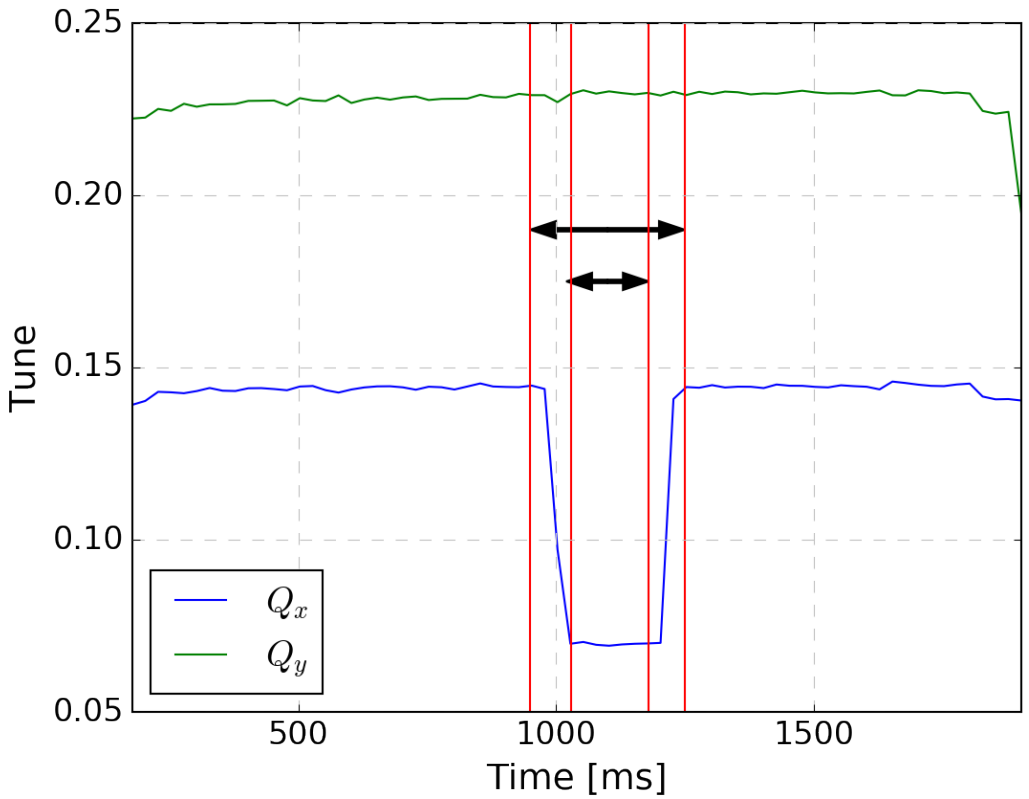

Figure 3: Wire scans are taken at the four time steps, indicated by red lines. They correspond to $950, 1030, 1180$ and 1250 [ms] each.

BPM around tune step

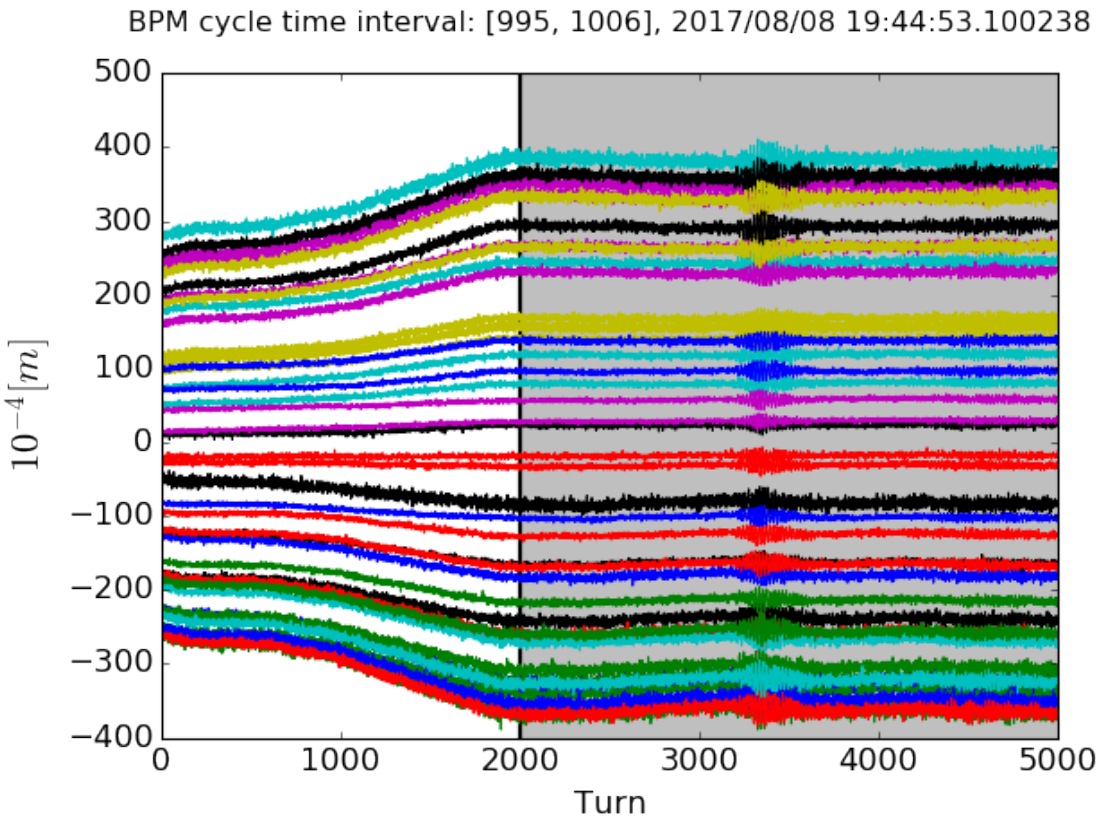

Figure 4: Beam centroid position on all BPMs during first step at around 1s cycle time. The grey area indicates the simulation region. The small excitation after around 3000 ms was done on purpose to check the tune.

Recall: Dispersion near the integer

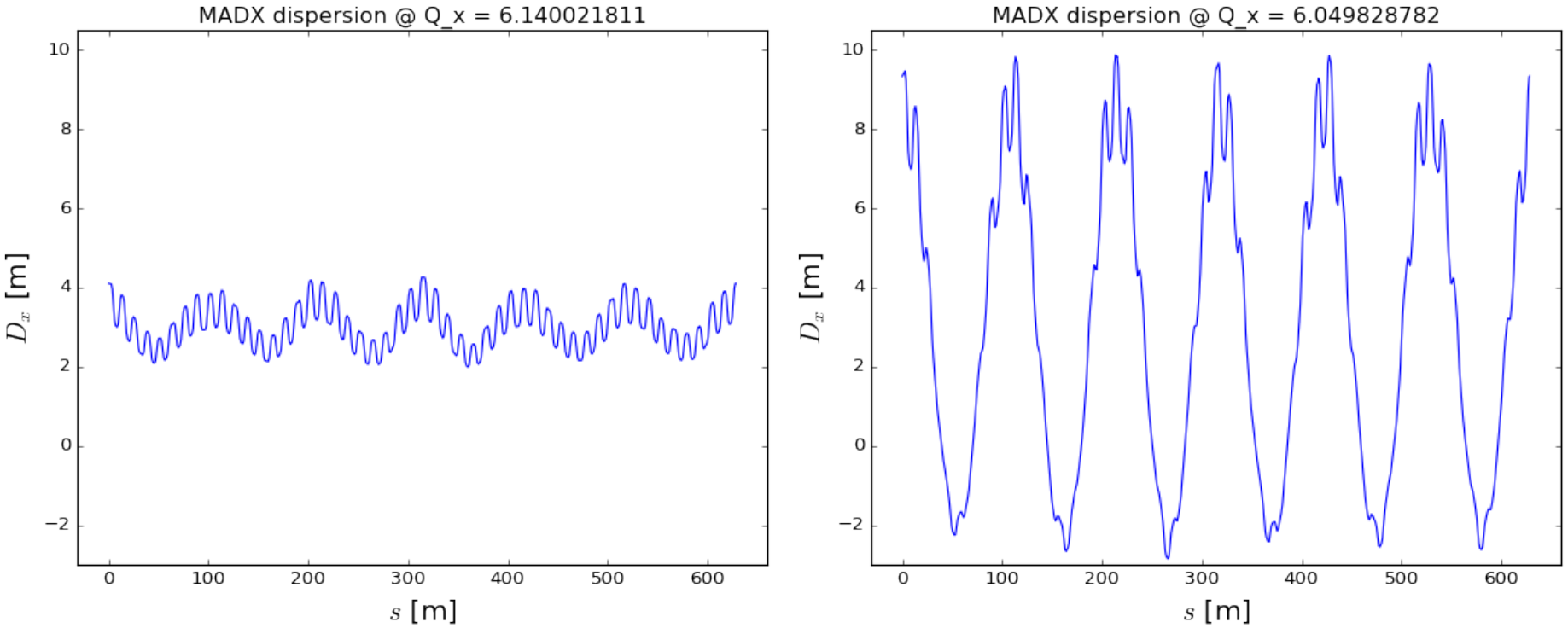

Figure 5: Dispersion at $Q_x = .140$ (left) and $Q_x = .050$ (right) predicted by MAD-X for the bare lattice (i.e. without SC).

Dispersion measurement

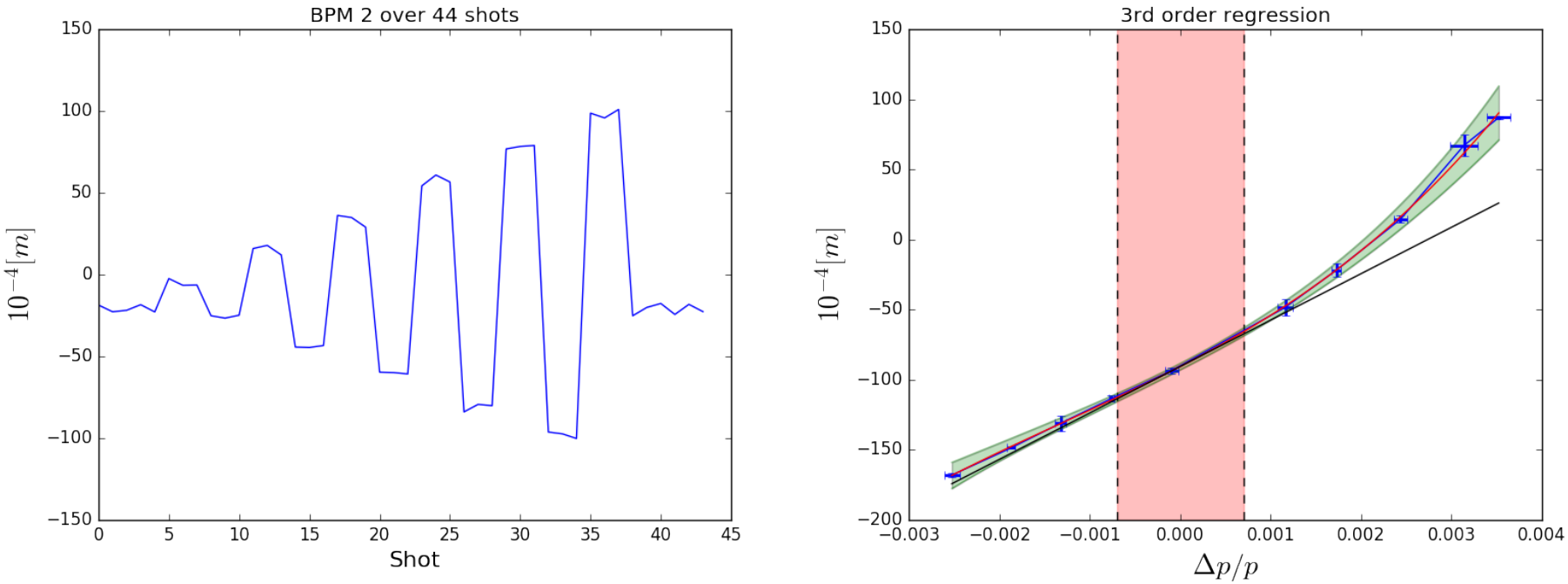

Figure 6: Sketch of dispersion measurement for a particular BPM. The pink area indicates the longitudinal RMS size of the bunch.

Dispersion measurement, p. 2

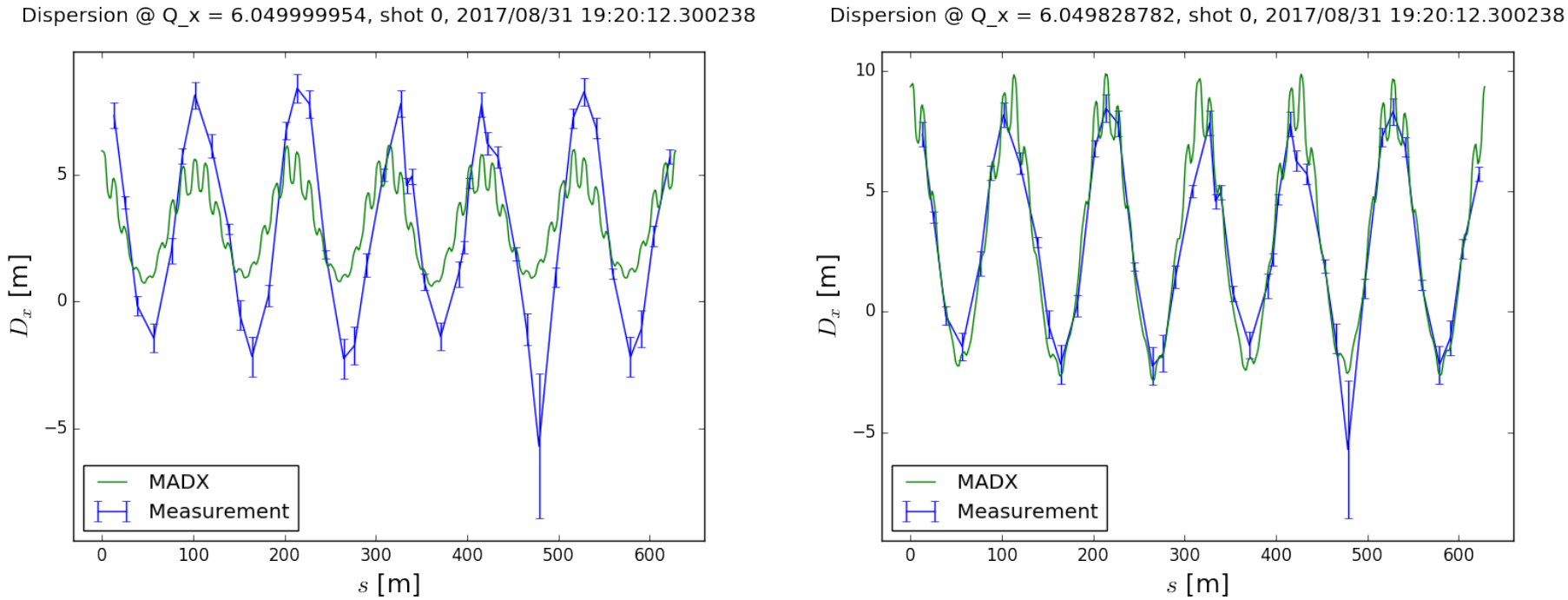

Figure 7: Effect of using a suitable horizontal correction kicker to adjust the measured dispersion, determined by first-order regression, to the MAD-X model ($20 \cdot 10^{10}$ setup).

Particle generation

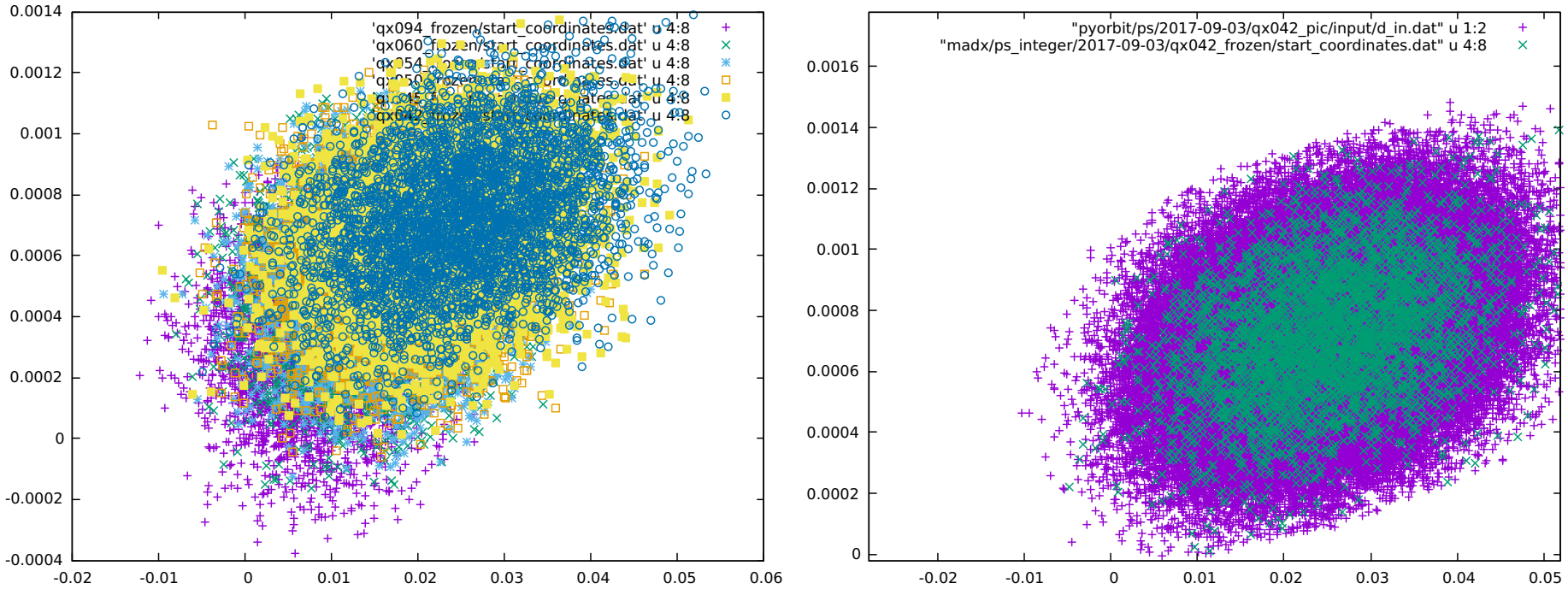

Figure 8: Start distributions taking into account the optics, including the change in the closed orbit due to dispersion. Left: (x, p_x) phase space for various working points in the MAD-X simulations. Right: Comparison between the PyOrbit and the MAD-X distributions for the $Q_x = 0.042$ working point ($30 \cdot 10^{10}$ setup).

Emittance evolution

Situation for the $30 \cdot 10^{10}$ case.

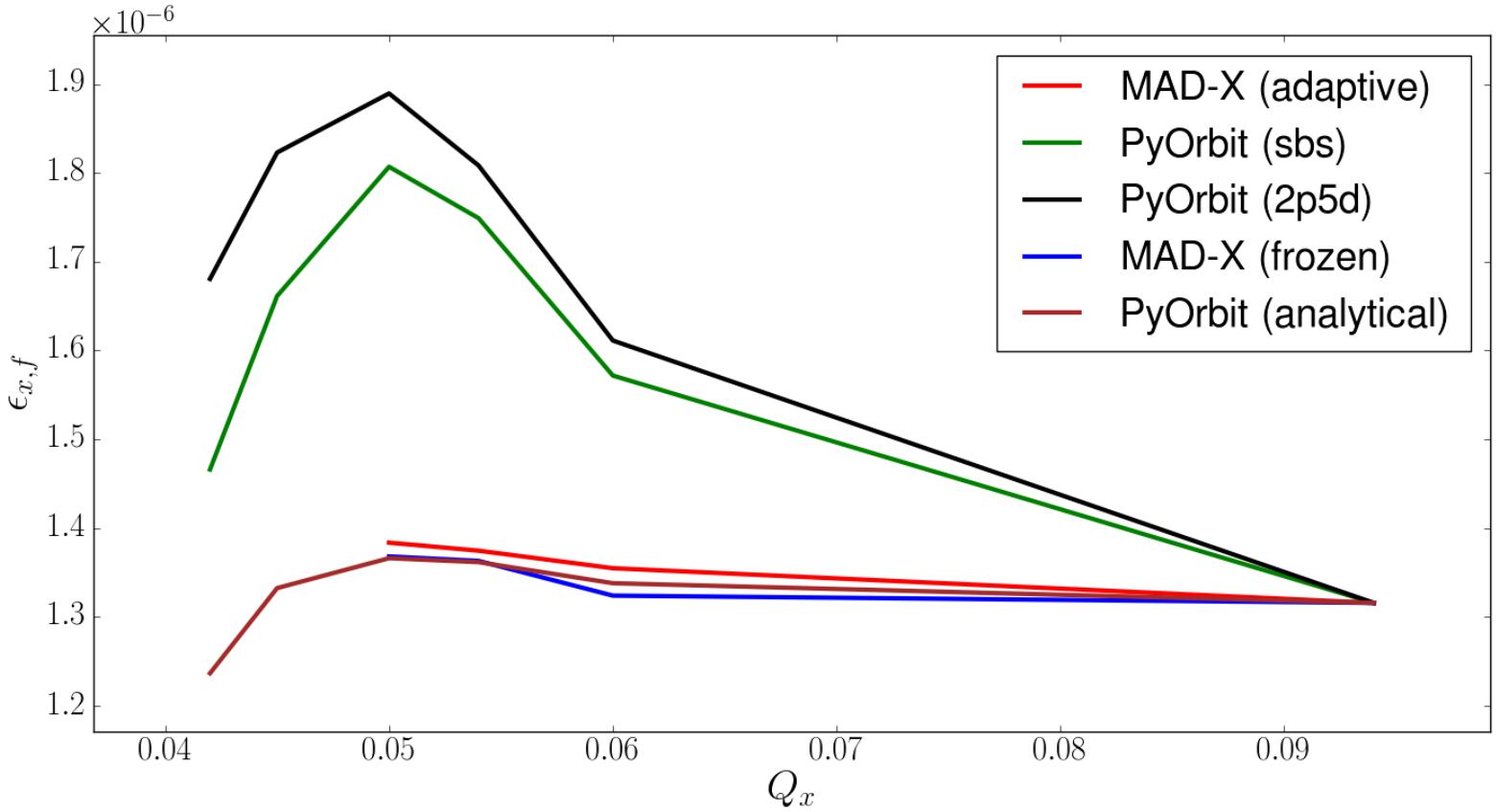

Figure 9: Emittance situation vs. working point for all 5 codes after 400 turns.

Experiment

Situation for the $30 \cdot 10^{10}$ case.

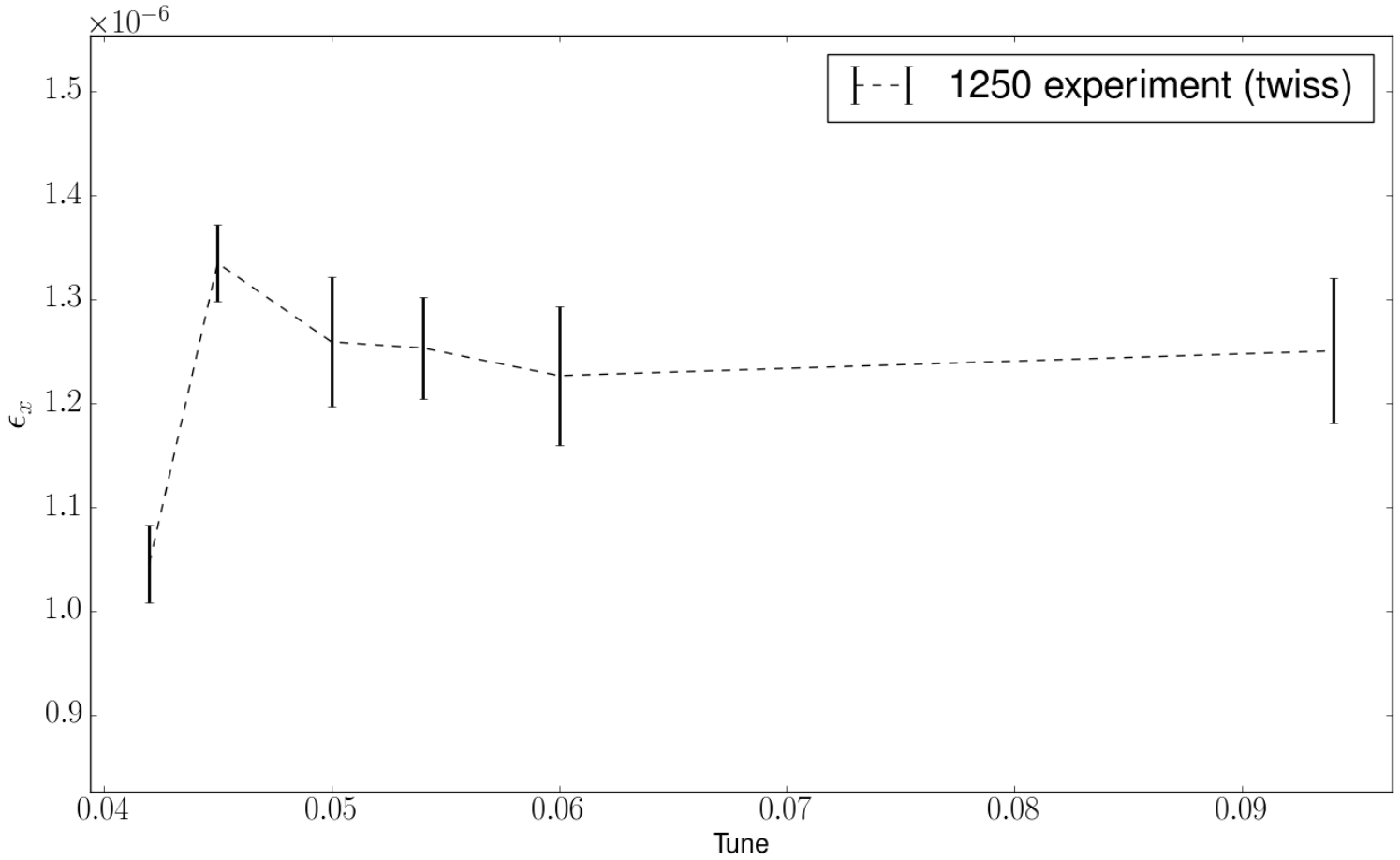

Figure 10: Emittance measured vs. working point after 1250 ms.

Emittance evolution

Situation for the $30 \cdot 10^{10}$ case.

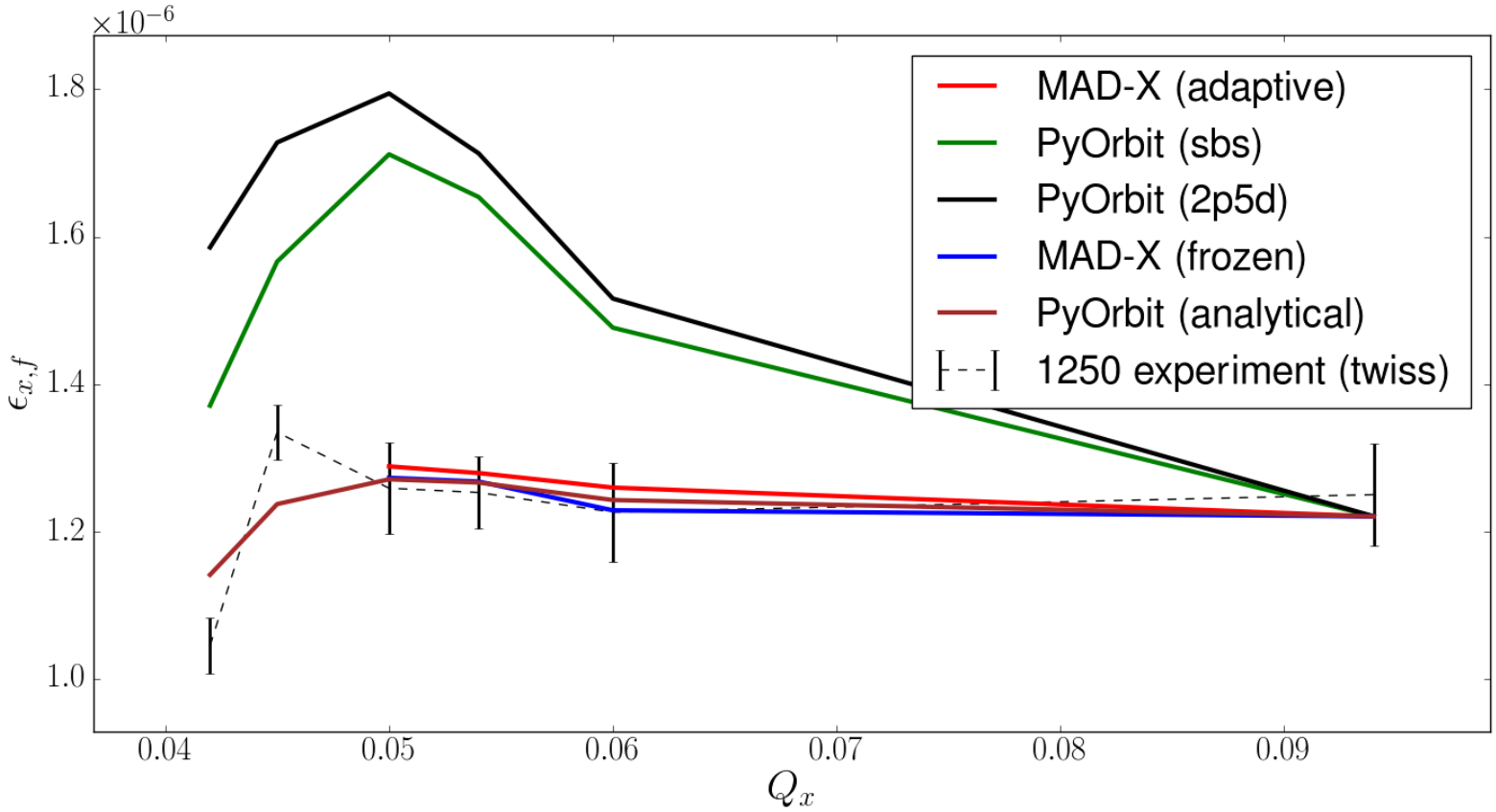

Figure 11: Emittance situation vs. working point for all 5 codes after 400 turns.

Investigating reason of PIC blow up ...

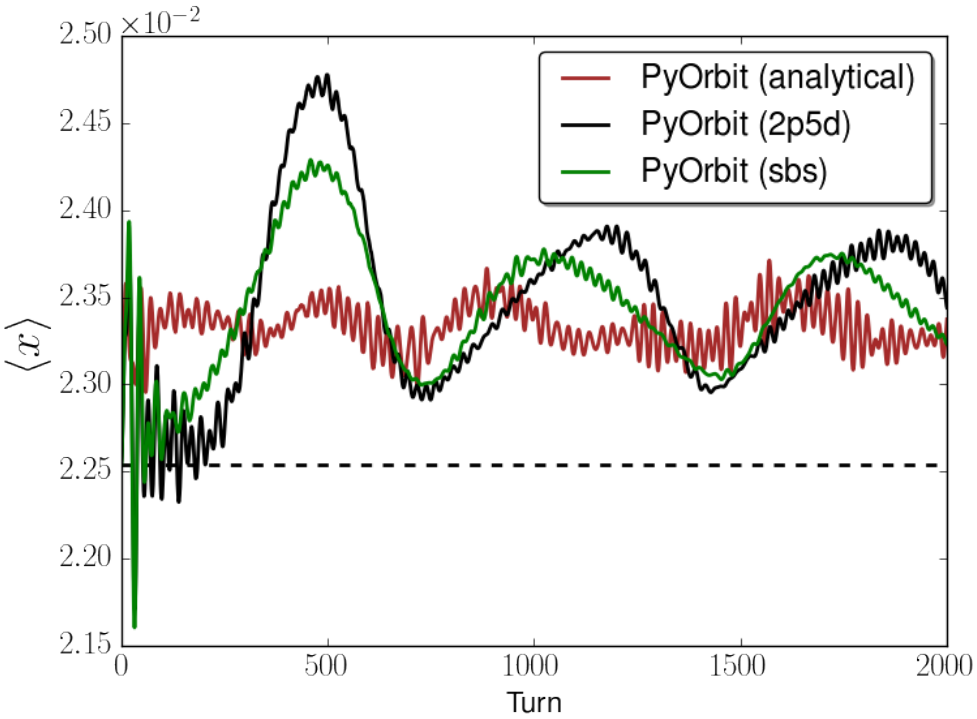

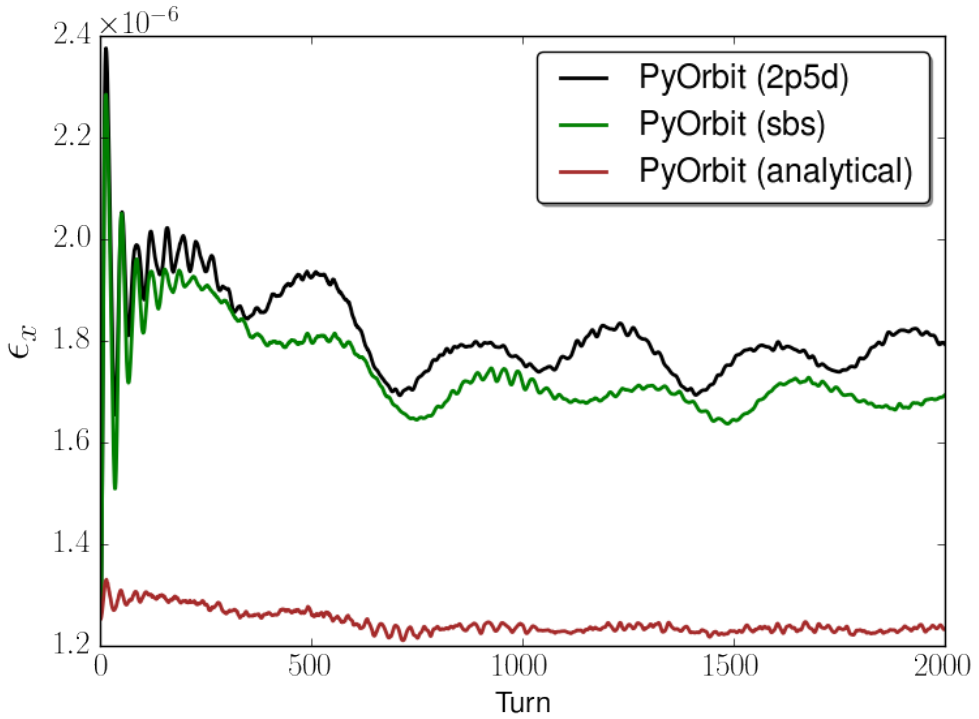

Figure 12: Mismatch issue currently under investigation, affecting in particular the PIC codes. The data shows the $Q_x = 0.054$ case, where the dashed black line indicates the closed orbit from MAD-X twiss. Right: Corresponding emittance evolution in x-direction.

Investigating reason of PIC blow up ...

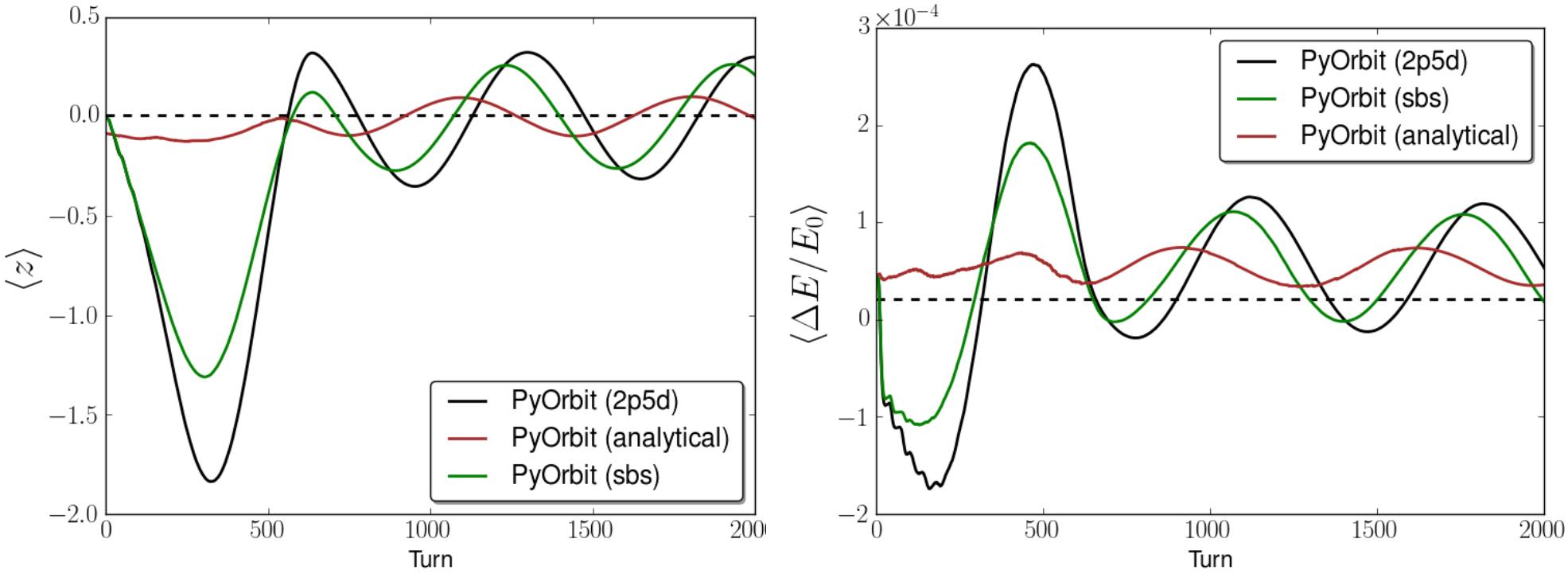

Figure 13: Longitudinal plane of the $Q_x = 0.054$ case.

Dispersion measurement, revisited

Furthermore:

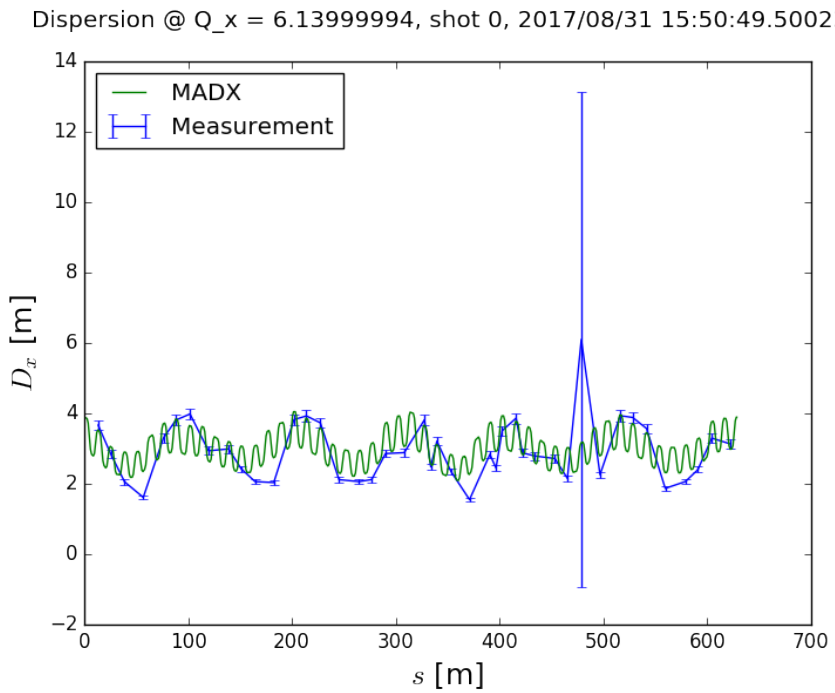

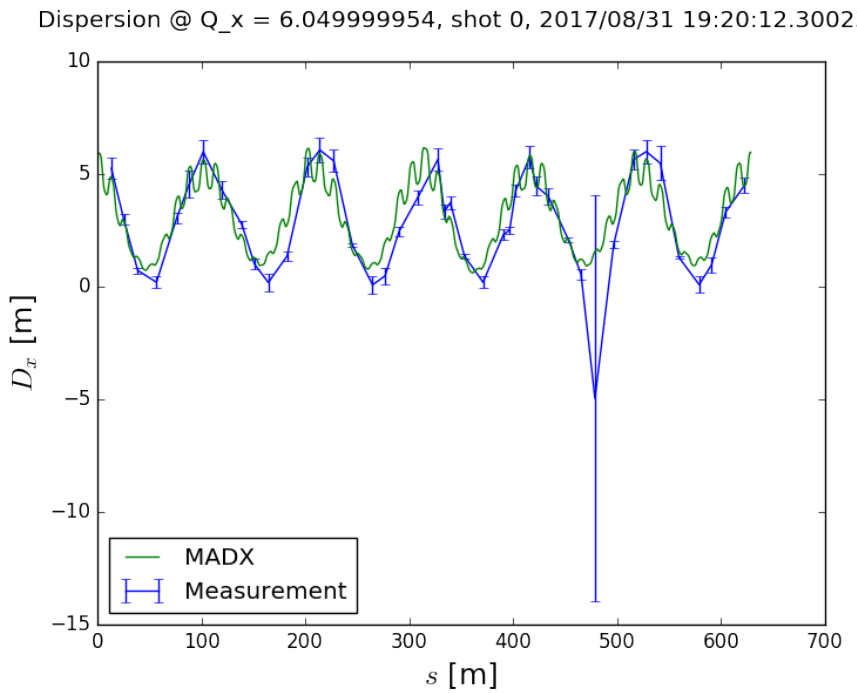

Figure 14: Uncorrected model seems to be closer to the measurements with 3rd order regression; left: nominal WP for $20 \cdot 10^{10}$ setup, right: same setup at $Q_x = 0.050$.

Conclusions

- Benchmarking between MAD-X and PyOrbit, and in particular emittance calculations, were done by means of 6D linear normal form maps, dealing with the pure tracking data of MAD-X and the covariance matrices of PyOrbit.
- Start distribution requires careful setup to avoid artificial emittance blow-up due to filamentation effects coming from changes in the closed-orbit dependent on the distance to the integer.
- Higher-order regression analysis is now investigated over all WPs to improve the PS model.
- A mismatch as the possible source for the short-term emittance blow-up is identified and going to be adressed in the near future.

Summary of simulation parameters

- Gaussian-like beam.
- Single bunch, 4k MP for MAD-X frozen/adaptive and 100k MP for the PIC codes.
- Grid points: $64 \times 64 \times 30$ for sbs and $64 \times 64 \times 20$ for 2p5d.
- Tunes:

$20 \cdot 10^{10}$	Q_x	.140	.060	.056	.050	.045	.040
	Q_y	.228	.228	.230	.230	.227	.226
$30 \cdot 10^{10}$	Q_x	.094	.060	.054	.050	.045	.042
	Q_y	.243	.243	.243	.241	.243	.245

p_0	2.14 [GeV]	
ϵ_x	$9.05 \cdot 10^{-7}(20 \cdot 10^{10})$	$1.316 \cdot 10^{-6}\,(30 \cdot 10^{10})$
ϵ_y	$5.45 \cdot 10^{-7}(20 \cdot 10^{10})$	$6.687 \cdot 10^{-7}\,(30 \cdot 10^{10})$
V_{RF}	25.3 [kV]	
h	8	
Q'_x	-5.693 (nWP at $30 \cdot 10^{10}$)	-4.742 (Measurement)
Q'_y	-7.553 (nWP at $30 \cdot 10^{10}$)	-7.279 (Measurement)

Extra material

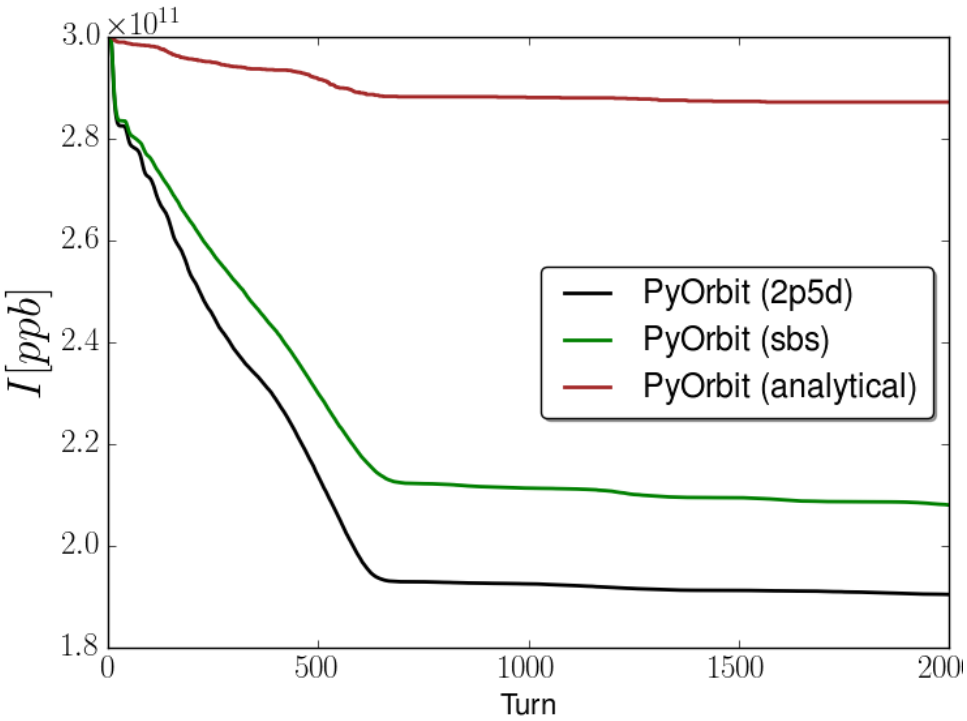

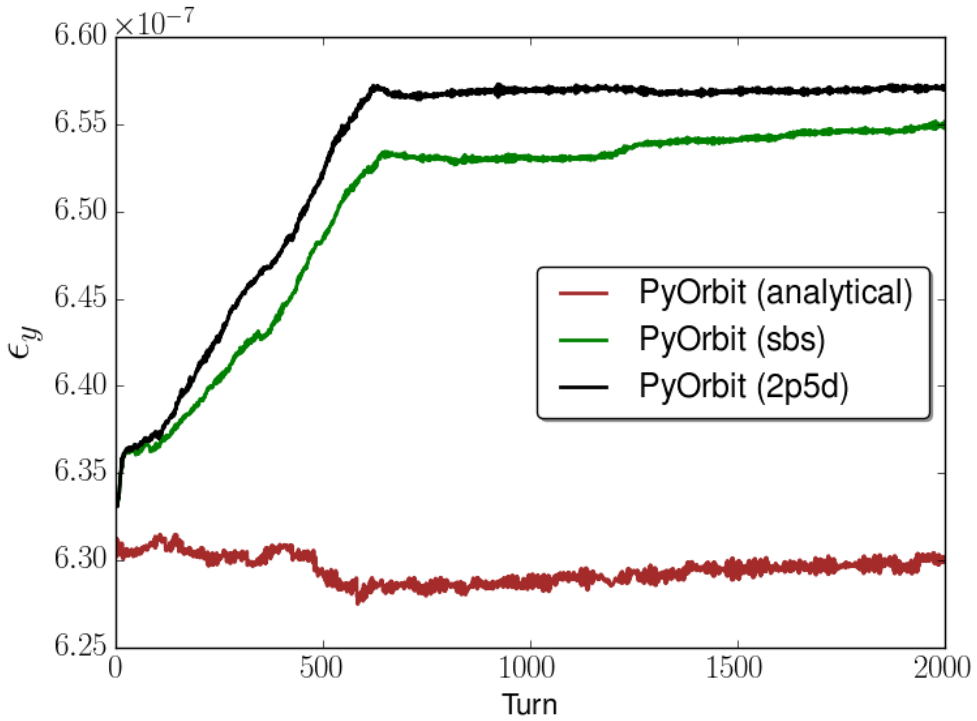

Figure 15: Intensity and ϵ_y of the case in Fig. 13.

Extra material, p. 2

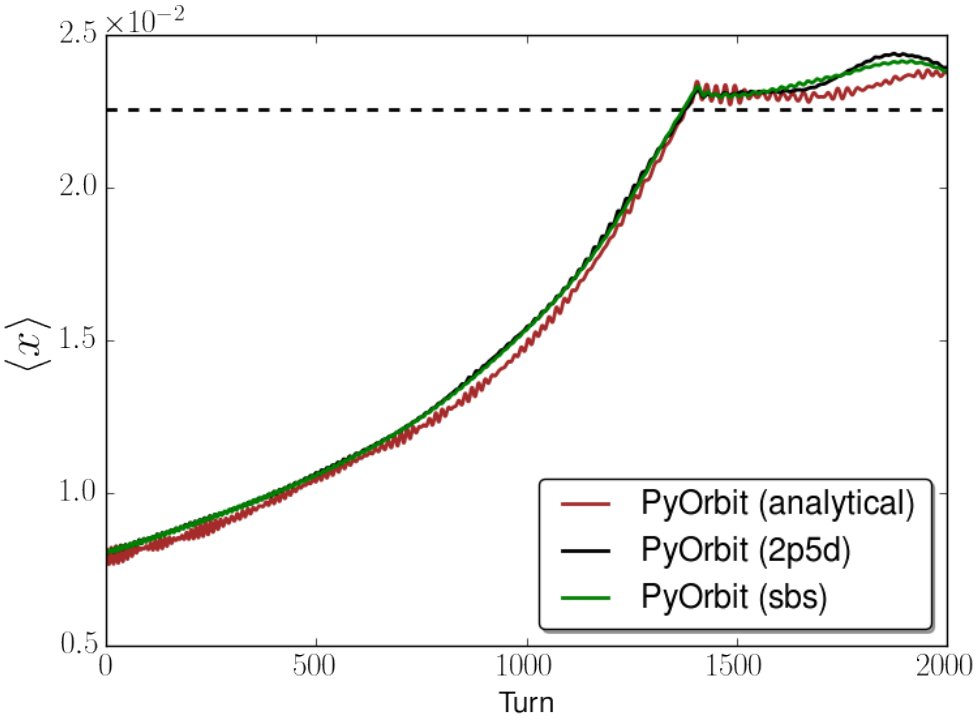

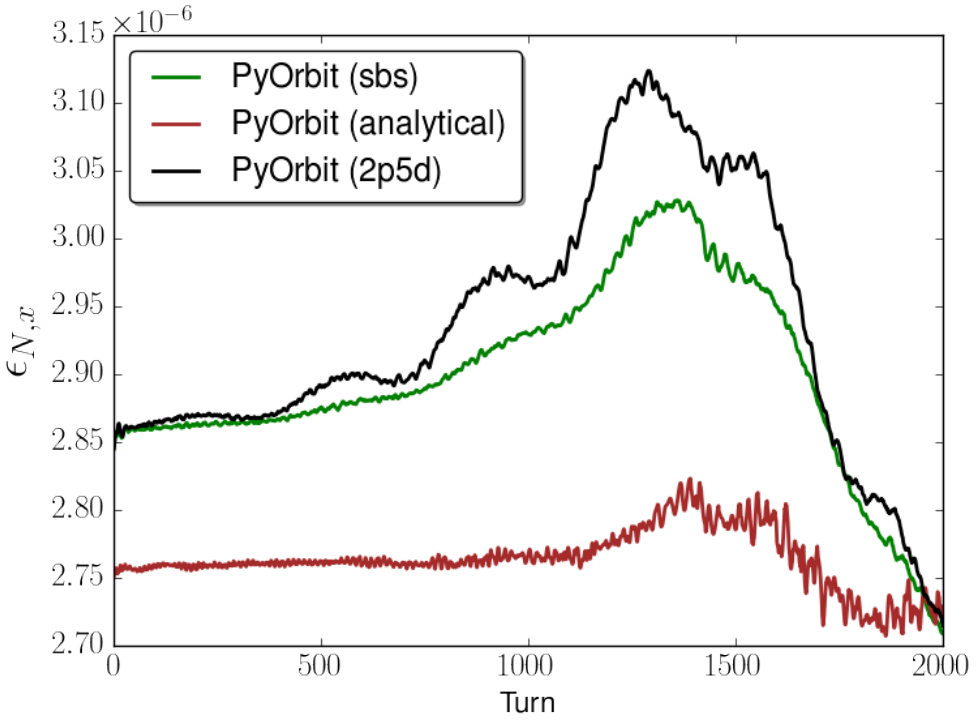

Figure 16: Beam centroid and emittance evolution as in Fig. 12, now ramping from the nominal WP towards $Q_x = 0.045$.

Beam centroid motion

However there is an interesting side effect of mismatch ...

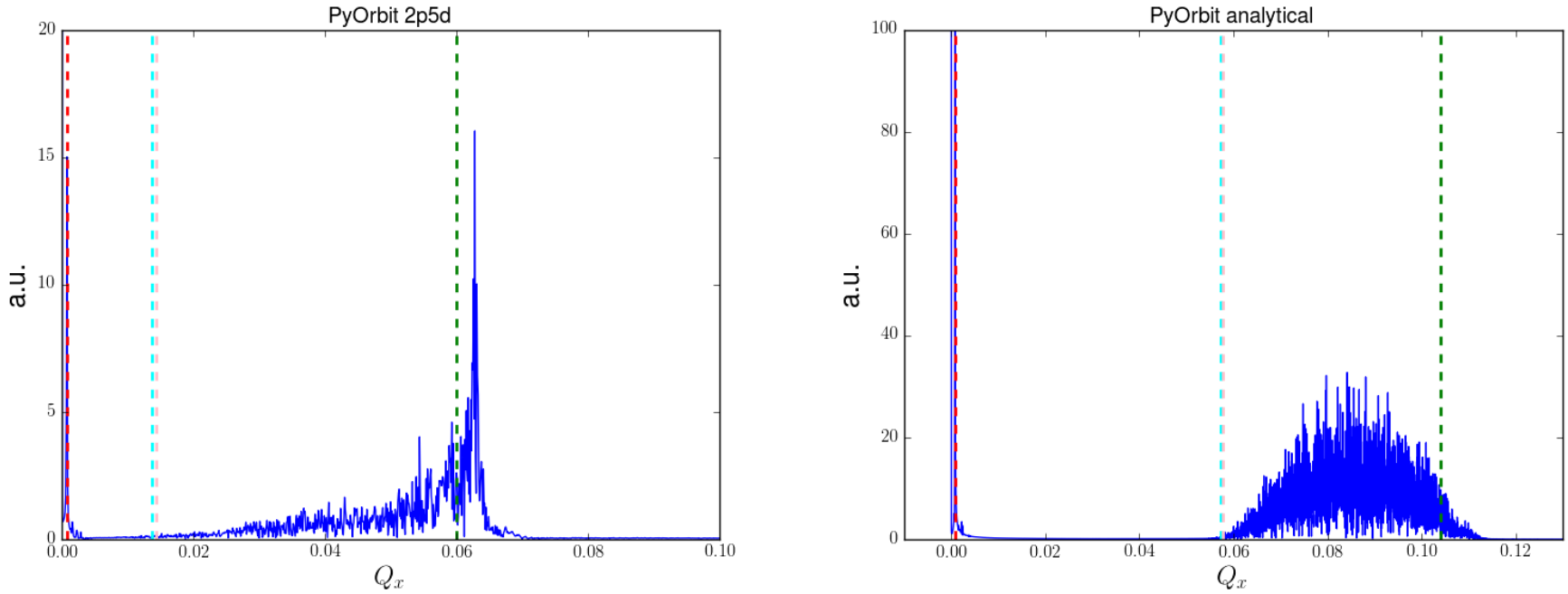

Figure 17: If mismatched, the beam centroid begin to perform oscillations. Bare tune of the lattices, which can be explained by Newton's 3rd law. Incoh. tune shift obtained by MAD-X SC as a result of the nonlinear beam-beam elements.